Detection of Sinkhole Precursors through SAR Interferometry: Radar and Geological Considerations

Journal:	*Geoscience and Remote Sensing Letters*
Manuscript ID	Draft
Manuscript Type:	Letters
Sub-topic:	Surface and Subsurface Properties
Date Submitted by the Author:	n/a
Complete List of Authors:	Theron, Andre; Council for Scientific and Industrial Research, Meraka; Stellenbosch University, Department of geography and environmental studies Engelbrecht, Jeanine; Council for Scientific and Industrial Research, Meraka Institute Kemp, Jaco; Stellenbosch University, Geopgraphy and Environmental Studies Kleynhans, Waldo; University of Pretoria, Electrical, Electronic and Com-pElectrical, Electronic and Com- puter Engineeringuter Engineering Turnbull, Terrence; South African Air Force, Air Command
Key Words:	Interferometry, Synthetic aperture radar, Geology, Hazardous areas

Detection of Sinkhole Precursors through SAR Interferometry: Radar and Geological Considerations

Andre Theron, *Member, IEEE*, Jeanine Engelbrecht, *Member, IEEE*, Jaco Kemp, *Member, IEEE*, Waldo Kleynhans, *Member, IEEE*, and Terrence Turnbull

***Abstract*— Sinkholes are an unpredictable geohazard that endangers life and property in dolomitic terrains. Sinkholes are a significant threat in Gauteng, South Africa's most populated and urbanised province. Small-scale surface subsidence is frequently present prior to the collapse of a sinkhole. Therefore, the presence of precursory surface deformation can be exploited to develop early warning indicators. Spaceborne SAR interferometry (DInSAR) is able to monitor small-scale surface deformation over large areas and can be used to detect and measure precursors to sinkhole development. This paper investigates the use of conventional DInSAR approaches to detect sinkhole precursors in the Gauteng Province. Twenty stripmap acquisitions of TerraSAR-X and TanDEM-X were acquired over a period of a full year. DInSAR results revealed the presence of 3 previously unknown deformation basins, one of which could be confirmed by subsequent field investigations. Furthermore, a water supply pipeline ruptured 6 months after the initial observation. The early detection of the deformation, therefore, provided a viable early warning to landowners who were unaware of the subsidence. Detected deformation basins were between 40 m and 100 m in diameter. The maximum displacement measured was 7 cm over 55 days. Despite the successful detection, 7 sinkhole events occurred in the observation period for which no deformation could be detected. The results indicate that high-resolution, X-band interferometry is able to monitor dolomite-induced instability in an urban environment. However, considerations related to SAR interferometry and physical sinkhole properties need to be addressed before DInSAR can be used in an operational early warning system.**

***Index Terms*—Early warning, Interferometry, SAR, Sinkhole, TerraSAR-X**

This paper was submitted for review on 15 September 2016 and was supported financially by the CSIR Meraka institute studentship program.

A. Theron (orcid.org/0000-0001-7446-6071) is with the Meraka Institute at the Council for Scientific and Industrial Research, Pretoria, Gauteng, South Africa, and at the Department of Geography and Environmental Studies at the Stellenbosch University, Western Cape, South Africa (Corresponding author email: atheron1@csir.co.za)

J. Engelbrecht (orcid.org/0000-0003-3764-4582) and Waldo Kleynhans is with the Meraka Institute at the Council for Scientific and Industrial Research, Pretoria, Gauteng, South Africa (e-mails: jengelbrecht@csir.co.za wkleynhans@csir.co.za).

J. Kemp (orcid.org/0000-0002-7954-2093) is with the Department of Geography and Environmental Studies at the Stellenbosch University, Western Cape, South Africa (e-mail: jkemp@sun.ac.za).

Terrence Turnbull is at the South African Air force (e-mail: tvturnbull@gmail.com)

I. Introduction

SINKHOLE formation occurs where the bedrock comprises of highly soluble evaporites or calcium carbonates such as dolomite or limestone. Subsurface cavities are formed mainly due to groundwater extraction or the ingress of water, often from leaking services or poor storm water drainage. Both ultimately lead to the erosion of weathered roof material into cavities and the subsequent collapse of the roof strata. Sinkholes are a growing concern globally due to increasing urbanisation and development on susceptible areas [1]. Although sinkholes appear with little warning, the appearance of tension cracks, cracks in infrastructure and surface subsidence are often early warning signs of sinkhole development. Such surface deformation occurs weeks to months before sinkhole formation as the erosion of the roof material causes upward migration of the cavity [2]. Sinkhole formation is by nature abrupt and the location of underground cavities is frequently unknown. It is, therefore, challenging to identify and analyse the associated small-scale precursory deformation. Furthermore, in situ monitoring of large areas is not feasible.

Satellite-based Synthetic Aperture Radar (SAR) systems are a valuable and proven tool in deformation detection and monitoring due to their frequent repetition time, large swath coverage and high precision. Sinkholes are more challenging to detect than larger scale deformation features due, in part, to their small size and likely non-linear deformation rate. Recent research has indicated that precursory surface subsidence can occur and that differential interferometry techniques (DInSAR) can accurately detect it months to years before the event (see [2]–[5]). It has however been found that some collapse sinkholes did not exhibit precursory subsidence and not all deformation events lead to collapse events [6]. Despite a need for more research there is optimism that reliable sinkhole precursor detection using DInSAR techniques, especially in urban areas, are cost effective and feasible [7]–[12]. Available research is based on specific radar systems and only a limited number of sinkhole events (under local geologic conditions). There is, therefore, a strong incentive to apply this technology to various subsidence hazard-prone regions of the world, particularly in the susceptible urban areas of South Africa.

An estimated 25% of the Gauteng Province of South Africa is underlain by dolomite. There have been over 3000 sinkhole related events over the last 60 years, resulting in the loss of lives and damage to property exceeding 1 Billion Rands (approx. 70 million USD) [13]. This paper explores the ability of DInSAR to detect precursory subsidence in a sinkhole prone urban area in the Gauteng Province. The data and processing framework are provided in Section II. The results are presented in Section III and are centered on a case study. A discussion of challenges to reliable detection identified during the study is presented in Section VI.

II. DATA AND METHODS

This study used the TerraSAR-X and TanDEM-X sensors collecting repeat-pass data in Stripmap mode in HH polarisation and ~40° incidence angle. The system's high spatial resolution (~3 m), frequent revisit time (11 days) and sensitivity to deformation made it a promising platform for this investigation. Historically, sinkholes in the study area have been between 2 m and 15 m in size and high spatial resolution radar data was, therefore, an important consideration [13]. Data was acquired from January 2015 to January 2016 with revisit times of between 11 and 77 days, resulting in 21 interferometric pairs (Table I). Perpendicular baselines were generally low with a maximum of 365m between 2015/02/09 and 2015/04/27.

TABLE I
TERRASAR-X DATASET PROPERTIES

Acquisition date	Temporal baseline (days)[1]	Perpendicular baseline (metres)[1]
2015/01/29	11	217
2015/02/09	77	365
2015/04/27	11	341
2015/05/08	33	23
2015/06/10	11	41
2015/06/21	11	10
2015/07/02	11	69
2015/07/13	33	14
2015/08/15	22	3
2015/09/06	11	73
2015/09/17	11	4
2015/09/28	11	192
2015/10/09	11	12
2015/10/20	11	295
2015/10/31	11	271
2015/11/11	11	176
2015/11/22	11	184
2015/12/03	11	71
2015/12/14	22	57
2016/01/05	22	118
2016/01/27	N/A	N/A

[1]Relative to the following acquisition.

Conventional differential interferometry techniques were used to derive surface deformation maps of the area under investigation. The topographic phase was modelled using the 'SUDEM' (5m resolution, 10.2 m vertical RMSE and EGM96 geoid subtracted). This is an integration of the SRTM-1 and the South African national contour and point height data sets and allows for improved topographic modelling [14]. Single look complex images were co-registered (to accuracies < 0.1 pixels) before interferogram generation. The interferograms were filtered using an adaptive Goldstein filter and unwrapped using the minimum cost flow algorithm using coherence as a weighting function. Vertical displacement maps were calculated under the assumption that precursory subsidence in this environment would primarily be vertical.

Ancillary data used for analysis of the results include rainfall accumulation at a station central to the study area and an independent sinkhole inventory provided by the Council for Geoscience, South Africa. The inventory is continuously updated by local authorities and was used to assist in accuracy assessment and verification of the DInSAR results.

III. RESULTS

During the DInSAR observation period, seven sinkhole events, as outlined in Table II, were recorded by the Council for Geoscience. It should be noted that, in some cases, the size of the sinkhole or subsidence feature could not be recorded due to a lack of access to the site where the incident occurred. There are also significant uncertainties associated with the exact date of the incident as shown in Table II. For each of the sinkhole events, the DInSAR results were examined to determine if precursory deformation could be observed. However, results showed that not one of these events was observed by conventional DInSAR on the TerraSAR-X data.

TABLE II
DETAILS OF SINKHOLE INVENTORY EVENTS

Date	Type	Possible cause	D_x^* (m)	D_y^* (m)	D_z^* (m)
Mar 2015	Sinkhole	Leaking pipe	N/A	N/A	N/A
2015	Subsidence	Leaking pipe	16	4	0.2
2015	N/A	Leaking pipe	N/A	N/A	N/A
2015	Subsidence	Leaking pipe	N/A	N/A	N/A
3 Jan 2016	Sinkhole	Leaking pipe	20	13	9
Jan 2016	Sinkhole	Leaking pipe	6	3	2
29 Jan 2016	Sinkhole & Subsidence	Leaking sewer pipe	N/A	N/A	N/A

* D_x is the major axis diameter, D_y the minor axis diameter and D_z the depth.

Further analysis of DInSAR results resulted in the identification of three deformation basins. All three events were detected between 2015/06/10 and 2015/08/15. One event was confirmed in the field (reported on in [15]) and is investigated in the following case study. The other two deformation basins were characterised by deformation of less than 5 cm and were less than 100 m in diameter, yet remain unconfirmed and are not further investigated here.

Confirmed Deformation Event

The differential interferograms and vertical displacement maps of the confirmed deformation event are presented in Fig. 1 and Fig. 2, respectively. The first subsidence observation between 2015/06/21 and 2015/07/02 revealed a basin of 60 m in diameter with a maximum deformation of 22.4 mm observed.

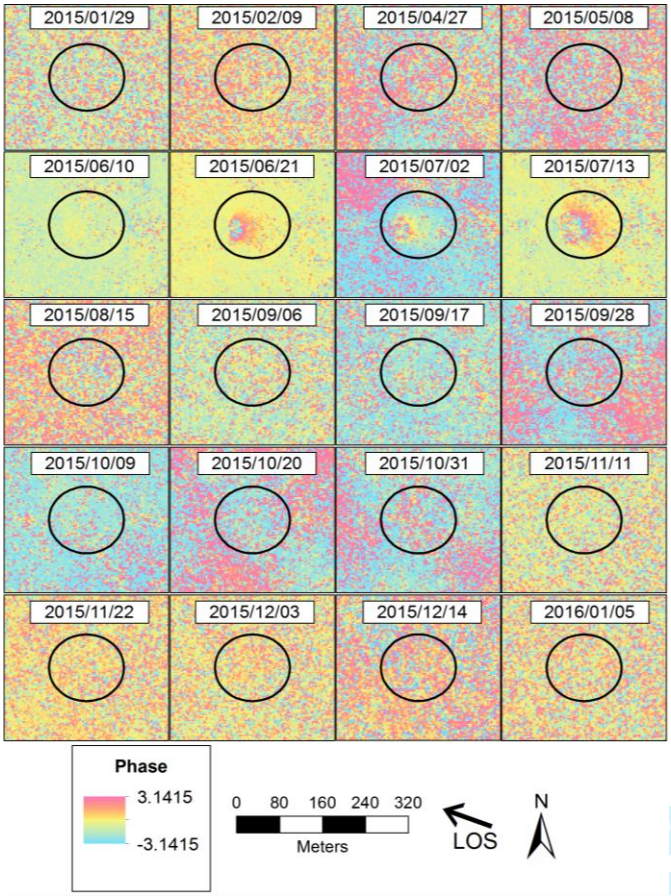

Fig. 1. Interferograms for the area surrounding the detected subsidence found within the black circle. Only the master date for each image pair is provided, the slave date of each image corresponds to the master date of the following image. The final slave date for the interferogram with the 2016/01/05 master is 2016/01/27. Deformation fringes are visible between 2015/06/21 and 2015/08/15

The basin remained similar in extent over the next detection between 2015/07/02 and 2015/07/13 with a maximum of 17.3 mm of deformation observed. The final detection period between 2015/07/13 and 2015/08/15 was associated with an increase in the extent of the basin to 70 m in diameter with a maximum of 42.2 mm of subsidence observed. No further deformation associated with this basin was detected on subsequent image pairs. However, it should be noted that a smaller, 40 m diameter, fringe signature was detected on two subsequent 11-day interferograms between 2015/10/20 and 2015/10/31 approximately 30 m away from this basin (not visible in Fig.1). This feature could not be distinguished from interferogram noise and was not confirmed in the field.

The temporal baseline of the final pair (2015/06/21 and 2015/08/15) is longer (33 days) compared to the two initial pairs with temporal baselines of 11 days, explaining the perceived increase in extent and magnitude of the deformation feature. The observed deformation basin reached a total extent of 80 m in diameter over a period of roughly 2 months with a maximum vertical subsidence of 66.7 mm (Fig. 2).

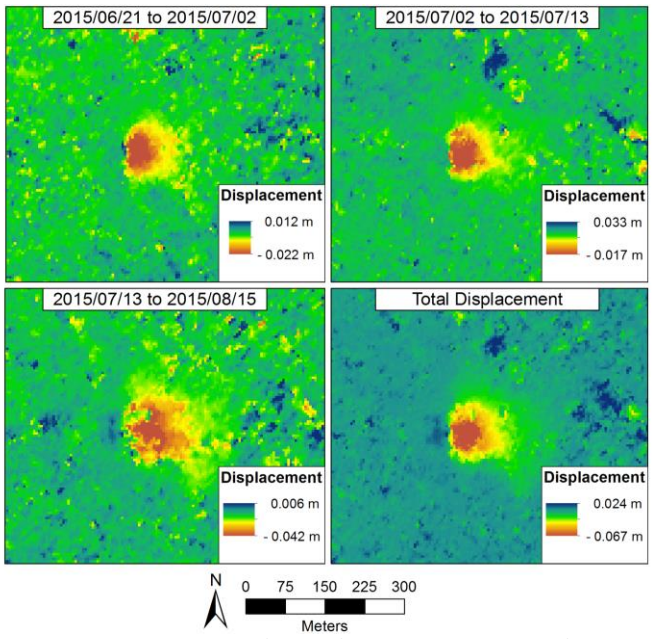

Fig. 2. Displacement maps of the deformation event derived from three interferograms as well as the sum of the three maps showing the total deformation detected over the period. The deformation gradient was steeper on the western periphery of the basin than on the east.

It is unlikely that the observed features were the result of residual topography due to the very low relief over the basin (less than 1 m change in elevation) and the large ambiguity heights for the pairs (453 m, 98 m and 393 m respectively). Residual atmospheric phase could also be ruled out due to the feature's small scale and high temporal correlation within the time series [16].

Field investigation of the basin revealed the presence of tension cracks tens of meters long on the western periphery of the basin, where the deformation gradient was the steepest. On 17 December 2015, a sinkhole of 0.5 m by 1.0 m was reported in the area, resulting in the rupturing of a water supply pipeline. Since the surface deformation was observed during a period associated with very little rainfall, it is postulated that the water supply pipeline was leaking for a period of several months prior to the deformation observations. The leaking servitude resulted in the formation of a cavity in the underlying dolomite. The surface subsidence observed using DInSAR observations were likely the result of the subsurface erosion of the roof strata into the cavity leading to localised surface instabilities. The eventual rupturing of the water supply pipeline was likely due to the increase of stress in the pipeline due to the deformation of the surface.

IV. DISCUSSION AND CONCLUSION

This paper presents promising results from a dolomite stability-monitoring project. The high spatiotemporal resolution and small perpendicular baselines of the TerraSAR-X data, as well as the urban nature of the study area, enabled accurate detection of surface instabilities. Using conventional DInSAR techniques and a time-series of data revealed the presence of a deformation basin. Subsequent field investigations suggest that the observed surface subsidence

was due to sinkhole formation, initiated by leaking water pipelines. However, the inability to detect any of the sinkhole events in the inventory reveals limitations to the technique and was investigated in more detail. Successful detection of sinkhole precursors through SAR interferometry is dependent on specific considerations that relate to 1) the properties of the SAR system and processing techniques applied to the data as well as 2) the geological signature of precursory deformation.

A. SAR and Processing Considerations

The resolution of the SAR system was identified as an important parameter for successful sinkhole precursor detection. It is known that deformation cannot reliably be detected by a single pixel [16] and the resolution of the SAR system, therefore, needs to be higher than the spatial scale of the deformation event. The largest sinkhole recorded in the inventory had a diameter of 20 m. This corresponds to approximately seven pixels on the TerraSAR-X system. Identifying deformation on less than 10 pixels is challenging [16] on interferograms and displacement maps resulting conventional DInSAR processing. The smallest confirmed detection during this study was in fact 60 m. Deformation-like fringe patterns 40 m in scale was observed but could not be distinguished from typical interferogram noise, a particular challenge for the X-band system. Advanced interferogram stacking techniques using point targets within the scattering cell [17] can compensate for this limitation. However, this reduces the spatial sampling density of the study area considerably and only point targets affected by the small-scale sinkhole deformation can be monitored. Processing workflows combining point targets and distributed scattering cells [17] is therefore recommended for sinkhole precursor detection.

Revisit time of the SAR is a further important consideration. A shorter revisit time (low temporal baseline) minimises the chance that deformation will exceed the deformation gradient. It furthermore results in a higher temporal sampling of the deformation feature, as well as providing a more timely early warning of imminent sinkhole events. Short temporal baselines are also important for reducing phase decorrelation between image acquisitions, particularly in vegetated areas [18].

Temporal decorrelation was found to be an important limitation to DInSAR sinkhole precursor detection. During this study, it was noted that deformation was only detected during periods of high average scene coherence. In fact, based on the limited detections during this study, an average-scene coherence threshold of 0.4 is regarded as the lower threshold of for successful detection in the area. The average scene coherence and its variation in the time series are presented in Fig. 3. There were two noteworthy periods where coherence was low during the study (Fig. 3). The first drop in coherence in the 2015/08/15 to 2015/09/06 interferogram resulted in uncertainty regarding the end date of detected deformation for the confirmed event discussed in Section III. This coherence reduction occurred during the middle of the dry season and was not related to increases in vegetation growth. Perpendicular and temporal baselines were also low for the interferometric pair in question.

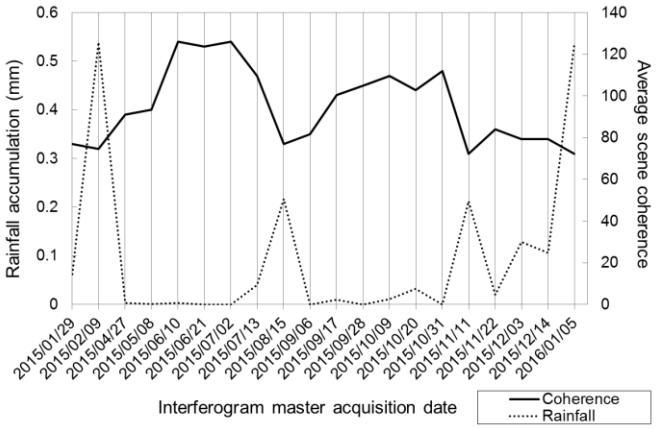

Fig. 3. Average global coherence and rainfall accumulation between the corresponding master and slave image acquisition dates. Two sudden drops in coherence are observed between master dates: 2015/08/15 and 2015/11/11. These are not associated with an increase in vegetation, temporal or perpendicular baselines but are related to rainfall accumulation.

However, as shown in Fig 3, rainfall accumulation between master and slave acquisitions was found to be associated with the sharp reduction in coherence. Rainfall leads to a disturbance and a dielectric change of the land surface which could have led to the coherence loss in this case.

SAR incidence angle and line of sight (LOS) is a final consideration influencing the DInSAR performance. A lower incidence angle leads to a higher spatial resolution, yet there is a real possibility of the subsidence signal being obscured by structures on the ground in the SAR's LOS [3]. Collecting data from descending and ascending satellite passes enables the observation of an area from the east and the west mitigating LOS challenges as well as providing the opportunity to collect three-dimensional deformation observations [4].

B. Geological Considerations

The final and more fundamental limitations are due to the nature of sinkhole precursors themselves. It is possible that no precursory deformation precedes a sinkhole development. The presence of chert bands in the study area, known for brittle failure with little warning [19], affects the potential for precursory deformation to be expressed. Furthermore, competent land cover types, like concrete, buildings or paved roads may be resistant to deformation and mask the expression of precursory deformation at the surface. Moreover, precursory deformation might only occur shortly before the sinkhole and deformation signatures are therefore masked by the sinkhole event depending on the temporal frequency of image acquisitions. Finally, the deformation magnitude may be too small to be detectable, especially in the presence of signal noise. In all these cases DInSAR would not be able to provide an early warning to sinkhole formation.

C. Concluding Remarks

The results of the investigation present evidence that

precursory deformation prior to sinkhole development can be detected by conventional DInSAR techniques. It is expected that SAR and processing limitations can be overcome with advanced processing techniques and appropriate SAR data selection. However, limitations related to the physical characteristics of sinkhole precursors remain a fundamental limitation to an early warning system based on ground deformation. Complementary ground-based methods are therefore expected to remain important for monitoring sinkhole prone land [9].

This investigation illustrates the opportunities and challenges to interferometric sinkholes precursor detection. There is a need for more evidence of DInSAR sinkhole precursors under different conditions. The resulting information will assist with the understanding of sinkhole dynamics as well as the operational limitations of DInSAR techniques in the context of a sinkhole early warning system.

Acknowledgment

The authors wish to thank the Council for Geoscience for providing the sinkhole inventory, the South African Weather Service for providing rainfall data and the Centre for Geographical Analysis at the Stellenbosch University for providing the SUDEM elevation model.

References

[1] J. De Waele, F. Gutiérrez, M. Parise, and L. Plan, "Geomorphology and natural hazards in karst areas: A review," *Geomorphology*, vol. 134, no. 1–2, pp. 1–8, 2011.

[2] L. Chang and R. F. Hanssen, "Detection of cavity migration and sinkhole risk using radar interferometric time series," *Remote Sensing of Environment*, vol. 147, pp. 56–64, 2014.

[3] E. Intrieri, G. Gigli, M. Nocentini, L. Lombardi, F. Mugnai, F. Fidolini, and N. Casagli, "Sinkhole monitoring and early warning: An experimental and successful GB-InSAR application," *Geomorphology*, vol. 241, pp. 304–314, 2015.

[4] C. E. Jones and R. G. Blom, "Pre-event and post-formation ground movement associated with the Bayou Corne sinkhole," in *Proceedings of the Sinkhole Conference*, 2015, pp. 415–422.

[5] R. N. Nof, G. Baer, A. Ziv, E. Raz, S. Atzori, and S. Salvi, "Sinkhole precursors along the Dead Sea, Israel, revealed by SAR interferometry," *Geology*, vol. 4, no. 9, pp. 1019–1022, 2013.

[6] M. L. Rucker, B. B. Panda, R. A. Meyers, and J. C. Lommler, "Using InSAR to detect subsidence at brine wells, sinkhole sites, and mines," *Carbonates and Evaporites*, vol. 28, pp. 141–147, 2013.

[7] Z. Stevanovic, M. Parise, D. Closson, F. Gutiérrez, and Z. Stevanović, "Anticipating and managing engineering problems in the complex karst environment," *Environmental Earth Sciences*, vol. 74, pp. 7823–7835, 2015.

[8] J. P. Galve, C. Castanada, F. Gutirezz, and G. Herrera, "Assessing sinkhole activity in the Ebro Valley mantled evaporite karst using advanced DInSAR," *Geomorphology*, vol. 229, pp. 30–44, 2015.

[9] A. Ozden, A. Faghri, M. Li, and K. Tabrizi, "Evaluation of Synthetic Aperture Radar satellite remote sensing for pavement and infrastructure monitoring," *Procedia Engineering*, vol. 145, pp. 752–759, 2016.

[10] K. E. Joyce, S. Samsonov, S. R. Levick, J. Engelbrecht, and S. Belliss, "Mapping and monitoring geological hazards using optical, LiDAR, and synthetic aperture RADAR image data," *Natural Hazards*, vol. 73, no. 2, pp. 137–163, 2014.

[11] M. Parise, "A procedure for evaluating the susceptibility to natural and anthropogenic sinkholes," *Georisk: Assessment and Management of Risk for Engineered Systems and Geohazards*, vol. 9, no. 4, pp. 1–14, 2015.

[12] K. Terwel and R. F. Hanssen, "Predicting structural disasters with Radar interferometry," in *Proceedings of the International Association for Bridge and Structural Engineering Congress*, 2015, pp. 824–831.

[13] S. Richardson, "Sinkhole and subsidence record in the chuniespoort group dolomite , Gauteng , South Africa," Master's thesis. Pretoria: University of Pretoria, Department of Geology, 2013.

[14] A. Van Niekerk, "Stellenbosch University Digital Elevation Model (SUDEM)," in *Product description report (2013 edition).*, 2014, pp. 1–13.

[15] A. Theron, J. Engelbrecht, J. Kemp, W. Kleynhans, and T. Turnbull, "Detection of sinkhole precursors through SAR interferometry : first results from South Africa," in *Proceedings of the IEEE International Geoscience and Remote Sensing Symposium*, 2016.

[16] D. Massonnet and K. L. Feigl, "Radar interferometry and its application to changes in the Earth's surface," *Reviews of Geophysics*, vol. 36, no. 4, p. 441, 1998.

[17] A. Ferretti, A. Fumagalli, F. Novali, C. Prati, F. Rocca, and A. Rucci, "A new algorithm for processing interferometric data-stacks: SqueeSAR," *IEEE Transactions on Geoscience and Remote Sensing*, vol. 49, no. 9, pp. 3460–3470, 2011.

[18] J. Engelbrecht, C. Musekiwa, J. Kemp, and M. R. Inggs, "Parameters affecting interferometric coherence-the case of a dynamic agricultural region," *IEEE Transactions on Geoscience and Remote Sensing*, vol. 52, no. 3, pp. 1572–1582, 2014.

[19] D. J. Avutia, "Analytical and numerical study of dolomite sinkholes in Centurion, South Africa," Master's thesis. Cape Town: University of Cape Town, Department of Civil Engineering, 2014.

Detection of Sinkhole Precursors through SAR Interferometry: Radar and Geological Considerations

Andre Theron, *Member, IEEE*, Jeanine Engelbrecht, *Member, IEEE*, Jaco Kemp, *Member, IEEE*, Waldo Kleynhans, *Member, IEEE*, and Terrence Turnbull

***Abstract*— Sinkholes are an unpredictable geohazard that endangers life and property in dolomitic terrains. Sinkholes are a significant threat in Gauteng, South Africa's most populated and urbanised province. Small-scale surface subsidence is frequently present prior to the collapse of a sinkhole. Therefore, the presence of precursory surface deformation can be exploited to develop early warning indicators. Spaceborne SAR interferometry (DInSAR) is able to monitor small-scale surface deformation over large areas and can be used to detect and measure precursors to sinkhole development. This paper investigates the use of conventional DInSAR approaches to detect sinkhole precursors in the Gauteng Province. Twenty stripmap acquisitions of TerraSAR-X and TanDEM-X were acquired over a period of a full year. DInSAR results revealed the presence of 3 previously unknown deformation basins, one of which could be confirmed by subsequent field investigations. Furthermore, a water supply pipeline ruptured 6 months after the initial observation. The early detection of the deformation, therefore, provided a viable early warning to landowners who were unaware of the subsidence. Detected deformation basins were between 40 m and 100 m in diameter. The maximum displacement measured was 7 cm over 55 days. Despite the successful detection, 7 sinkhole events occurred in the observation period for which no deformation could be detected. The results indicate that high-resolution, X-band interferometry is able to monitor dolomite-induced instability in an urban environment. However, considerations related to SAR interferometry and physical sinkhole properties need to be addressed before DInSAR can be used in an operational early warning system.**

***Index Terms*—Early warning, Interferometry, SAR, Sinkhole, TerraSAR-X**

I. Introduction

SINKHOLE formation occurs where the bedrock comprises of highly soluble evaporites or calcium carbonates such as dolomite or limestone. Subsurface cavities are formed mainly due to groundwater extraction or the ingress of water, often from leaking

This paper was submitted for review on 15 September 2016 and was supported financially by the CSIR Meraka institute studentship program.

A. Theron (orcid.org/0000-0001-7446-6071) is with the Meraka Institute at the Council for Scientific and Industrial Research, Pretoria, Gauteng, South Africa, and at the Department of Geography and Environmental Studies at the Stellenbosch University, Western Cape, South Africa (Corresponding author email: atheron1@csir.co.za)

J. Engelbrecht (orcid.org/0000-0003-3764-4582) and Waldo Kleynhans is with the Meraka Institute at the Council for Scientific and Industrial Research, Pretoria, Gauteng, South Africa (e-mails: jengelbrecht@csir.co.za wkleynhans@csir.co.za).

J. Kemp (orcid.org/0000-0002-7954-2093) is with the Department of Geography and Environmental Studies at the Stellenbosch University, Western Cape, South Africa (e-mail: jkemp@sun.ac.za).

Terrence Turnbull is at the South African Air force (e-mail: tvturnbull@gmail.com)

services or poor storm water drainage. Both ultimately lead to the erosion of weathered roof material into cavities and the subsequent collapse of the roof strata. Sinkholes are a growing concern globally due to increasing urbanisation and development on susceptible areas [1]. Although sinkholes appear with little warning, the appearance of tension cracks, cracks in infrastructure and surface subsidence are often early warning signs of sinkhole development. Such surface deformation occurs weeks to months before sinkhole formation as the erosion of the roof material causes upward migration of the cavity [2]. Sinkhole formation is by nature abrupt and the location of underground cavities is frequently unknown. It is, therefore, challenging to identify and analyse the associated small-scale precursory deformation. Furthermore, in situ monitoring of large areas is not feasible.

Satellite-based Synthetic Aperture Radar (SAR) systems are a valuable and proven tool in deformation detection and monitoring due to their frequent repetition time, large swath coverage and high precision. Sinkholes are more challenging to detect than larger scale deformation features due, in part, to their small size and likely non-linear deformation rate. Recent research has indicated that precursory surface subsidence can occur and that differential interferometry techniques (DInSAR) can accurately detect it months to years before the event (see [2]–[5]). It has however been found that some collapse sinkholes did not exhibit precursory subsidence and not all deformation events lead to collapse events [6]. Despite a need for more research there is optimism that reliable sinkhole precursor detection using DInSAR techniques, especially in urban areas, are cost effective and feasible [7]–[12]. Available research is based on specific radar systems and only a limited number of sinkhole events (under local geologic conditions). There is, therefore, a strong incentive to apply this technology to various subsidence hazard-prone regions of the world, particularly in the susceptible urban areas of South Africa.

An estimated 25% of the Gauteng Province of South Africa is underlain by dolomite. There have been over 3000 sinkhole related events over the last 60 years, resulting in the loss of lives and damage to property exceeding 1 Billion Rands (approx. 70 million USD) [13]. This paper explores the ability of DInSAR to detect precursory subsidence in a sinkhole prone urban area in the Gauteng Province. The data and processing framework are provided in Section II. The results are presented in Section III and are centered on a case study. A discussion of challenges to reliable detection identified during the study is presented in Section VI.

II. DATA AND METHODS

This study used the TerraSAR-X and TanDEM-X sensors collecting repeat-pass data in Stripmap mode in HH polarisation and ~40° incidence angle. The system's high spatial resolution (~3 m), frequent revisit time (11 days) and sensitivity to deformation made it a promising platform for this investigation. Historically, sinkholes in the study area have been between 2 m and 15 m in size and high spatial resolution radar data was, therefore, an important consideration [13]. Data was acquired from January 2015 to January 2016 with revisit times of between 11 and 77 days, resulting in 21 interferometric pairs (Table I). Perpendicular

baselines were generally low with a maximum of 365m between 2015/02/09 and 2015/04/27.

TABLE I
TERRASAR-X DATASET PROPERTIES

Acquisition date	Temporal baseline (days)[1]	Perpendicular baseline (metres)[1]
2015/01/29	11	217
2015/02/09	77	365
2015/04/27	11	341
2015/05/08	33	23
2015/06/10	11	41
2015/06/21	11	10
2015/07/02	11	69
2015/07/13	33	14
2015/08/15	22	3
2015/09/06	11	73
2015/09/17	11	4
2015/09/28	11	192
2015/10/09	11	12
2015/10/20	11	295
2015/10/31	11	271
2015/11/11	11	176
2015/11/22	11	184
2015/12/03	11	71
2015/12/14	22	57
2016/01/05	22	118
2016/01/27	N/A	N/A

[1]Relative to the following acquisition.

Conventional differential interferometry techniques were used to derive surface deformation maps of the area under investigation. The topographic phase was modelled using the 'SUDEM' (5m resolution, 10.2 m vertical RMSE and EGM96 geoid subtracted). This is an integration of the SRTM-1 and the South African national contour and point height data sets and allows for improved topographic modelling [14]. Single look complex images were co-registered (to accuracies < 0.1 pixels) before interferogram generation. The interferograms were filtered using an adaptive Goldstein filter and unwrapped using the minimum cost flow algorithm using coherence as a weighting function. Vertical displacement maps were calculated under the assumption that precursory subsidence in this environment would primarily be vertical.

Ancillary data used for analysis of the results include rainfall accumulation at a station central to the study area and an independent sinkhole inventory provided by the Council for Geoscience, South Africa. The inventory is continuously updated by local authorities and was used to assist in accuracy assessment and verification of the DInSAR results.

III. RESULTS

During the DInSAR observation period, seven sinkhole events, as outlined in Table II, were recorded by the Council for Geoscience. It should be noted that, in some cases, the size of the sinkhole or subsidence feature could not be recorded due to a lack of access to the site where the incident occurred. There are also significant uncertainties associated with the exact date of the incident as shown in Table II. For each of the sinkhole events, the DInSAR results were examined to determine if precursory deformation could be observed. However, results showed that not one of these events was observed by conventional DInSAR on the TerraSAR-X data.

TABLE II
DETAILS OF SINKHOLE INVENTORY EVENTS

Date	Type	Possible cause	D_x^* (m)	D_y^* (m)	D_z^* (m)
Mar 2015	Sinkhole	Leaking pipe	N/A	N/A	N/A
2015	Subsidence	Leaking pipe	16	4	0.2
2015	N/A	Leaking pipe	N/A	N/A	N/A
2015	Subsidence	Leaking pipe	N/A	N/A	N/A
3 Jan 2016	Sinkhole	Leaking pipe	20	13	9
Jan 2016	Sinkhole	Leaking pipe	6	3	2
29 Jan 2016	Sinkhole & Subsidence	Leaking sewer pipe	N/A	N/A	N/A

* D_x is the major axis diameter, D_y the minor axis diameter and D_z the depth.

Further analysis of DInSAR results resulted in the identification of three deformation basins. All three events were detected between 2015/06/10 and 2015/08/15. One event was confirmed in the field (reported on in [15]) and is investigated in the following case study. The other two deformation basins were characterised by deformation of less than 5 cm and were less than 100 m in diameter, yet remain unconfirmed and are not further investigated here.

Confirmed Deformation Event

The differential interferograms and vertical displacement maps of the confirmed deformation event are presented in Fig. 1 and Fig. 2, respectively. The first subsidence observation between 2015/06/21 and 2015/07/02 revealed a basin of 60 m in diameter with a maximum deformation of 22.4 mm observed.

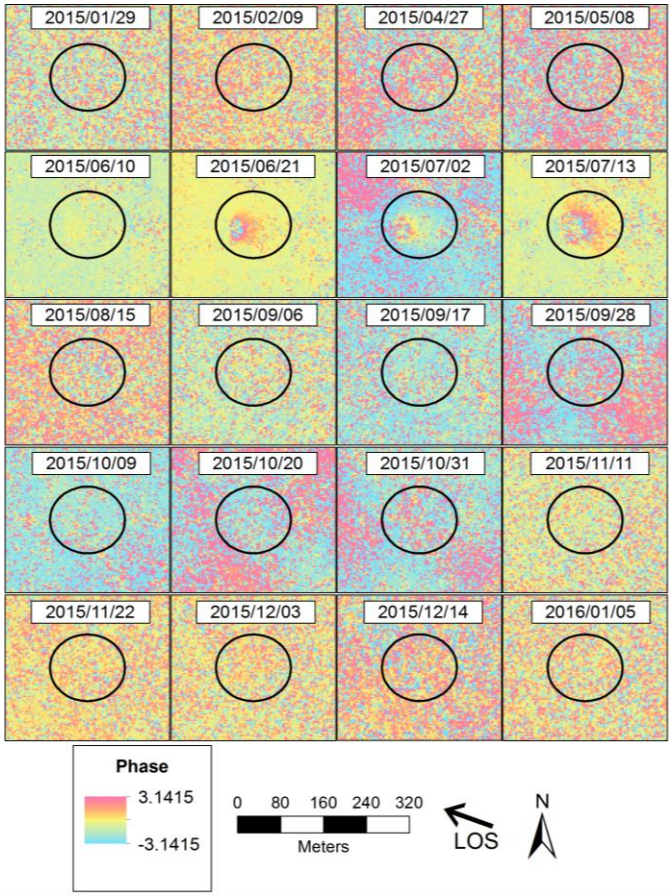

Fig. 1. Interferograms for the area surrounding the detected subsidence found within the black circle. Only the master date for each image pair is provided, the slave date of each image corresponds to the master date of the following image. The final slave date for the interferogram with the 2016/01/05 master is 2016/01/27. Deformation fringes are visible between 2015/06/21 and 2015/08/15

The basin remained similar in extent over the next detection between 2015/07/02 and 2015/07/13 with a maximum of 17.3 mm of deformation observed. The final detection period between 2015/07/13 and 2015/08/15 was associated with an increase in the extent of the basin to 70 m in diameter with a maximum of 42.2 mm of subsidence observed. No further deformation associated with this basin was detected on subsequent image pairs. However, it should be noted that a smaller, 40 m diameter, fringe signature was detected on two subsequent 11-day interferograms between 2015/10/20 and 2015/10/31 approximately 30 m away from this basin (not visible in Fig.1). This feature could not be distinguished from interferogram noise and was not confirmed in the field.

The temporal baseline of the final pair (2015/06/21 and 2015/08/15) is longer (33 days) compared to the two initial pairs with temporal baselines of 11 days, explaining the perceived increase in extent and magnitude of the deformation feature. The observed deformation basin reached a total extent of 80 m in diameter over a period of roughly 2 months with a maximum vertical subsidence of 66.7 mm (Fig. 2).

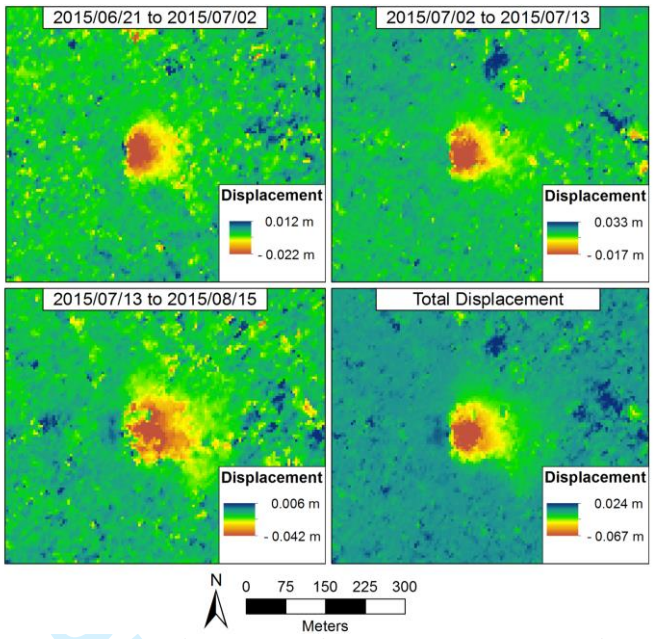

Fig. 2. Displacement maps of the deformation event derived from three interferograms as well as the sum of the three maps showing the total deformation detected over the period. The deformation gradient was steeper on the western periphery of the basin than on the east.

It is unlikely that the observed features were the result of residual topography due to the very low relief over the basin (less than 1 m change in elevation) and the large ambiguity heights for the pairs (453 m, 98 m and 393 m respectively). Residual atmospheric phase could also be ruled out due to the feature's small scale and high temporal correlation within the time series [16].

Field investigation of the basin revealed the presence of tension cracks tens of meters long on the western periphery of the basin, where the deformation gradient was the steepest. On 17 December 2015, a sinkhole of 0.5 m by 1.0 m was reported in the area, resulting in the rupturing of a water supply pipeline. Since the surface deformation was observed during a period associated with very little rainfall, it is postulated that the water supply pipeline was leaking for a period of several months prior to the deformation observations. The leaking servitude resulted in the formation of a cavity in the underlying dolomite. The surface subsidence observed using DInSAR observations were likely the result of the subsurface erosion of the roof strata into the cavity leading to localised surface instabilities. The eventual rupturing of the water supply pipeline was likely due to the increase of stress in the pipeline due to the deformation of the surface.

IV. DISCUSSION AND CONCLUSION

This paper presents promising results from a dolomite stability-monitoring project. The high spatiotemporal resolution and small perpendicular baselines of the TerraSAR-X data, as well as the urban nature of the study area, enabled accurate detection of surface instabilities. Using conventional DInSAR techniques and a time-series of data revealed the presence of a deformation basin. Subsequent field investigations suggest that the observed surface subsidence was due to sinkhole formation, initiated by leaking water pipelines. However, the inability to detect any of the sinkhole events in the inventory reveals limitations to the

technique and was investigated in more detail. Successful detection of sinkhole precursors through SAR interferometry is dependent on specific considerations that relate to 1) the properties of the SAR system and processing techniques applied to the data as well as 2) the geological signature of precursory deformation.

A. SAR and Processing Considerations

The resolution of the SAR system was identified as an important parameter for successful sinkhole precursor detection. It is known that deformation cannot reliably be detected by a single pixel [16] and the resolution of the SAR system, therefore, needs to be higher than the spatial scale of the deformation event. The largest sinkhole recorded in the inventory had a diameter of 20 m. This corresponds to approximately seven pixels on the TerraSAR-X system. Identifying deformation on less than 10 pixels is challenging [16] on interferograms and displacement maps resulting conventional DInSAR processing. The smallest confirmed detection during this study was in fact 60 m. Deformation-like fringe patterns 40 m in scale was observed but could not be distinguished from typical interferogram noise, a particular challenge for the X-band system. Advanced interferogram stacking techniques using point targets within the scattering cell [17] can compensate for this limitation. However, this reduces the spatial sampling density of the study area considerably and only point targets affected by the small-scale sinkhole deformation can be monitored. Processing workflows combining point targets and distributed scattering cells [17] is therefore recommended for sinkhole precursor detection.

Revisit time of the SAR is a further important consideration. A shorter revisit time (low temporal baseline) minimises the chance that deformation will exceed the deformation gradient. It furthermore results in a higher temporal sampling of the deformation feature, as well as providing a more timely early warning of imminent sinkhole events. Short temporal baselines are also important for reducing phase decorrelation between image acquisitions, particularly in vegetated areas [18].

Temporal decorrelation was found to be an important limitation to DInSAR sinkhole precursor detection. During this study, it was noted that deformation was only detected during periods of high average scene coherence. In fact, based on the limited detections during this study, an average-scene coherence threshold of 0.4 is regarded as the lower threshold of for successful detection in the area. The average scene coherence and its variation in the time series are presented in Fig. 3. There were two noteworthy periods where coherence was low during the study (Fig. 3). The first drop in coherence in the 2015/08/15 to 2015/09/06 interferogram resulted in uncertainty regarding the end date of detected deformation for the confirmed event discussed in Section III. This coherence reduction occurred during the middle of the dry season and was not related to increases in vegetation growth. Perpendicular and temporal baselines were also low for the interferometric pair in question.

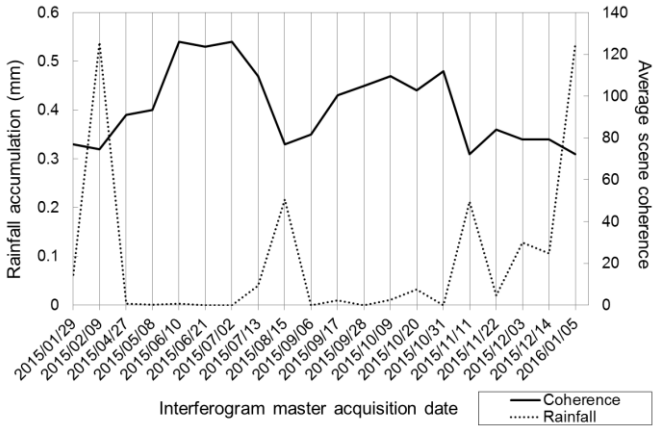

Fig. 3. Average global coherence and rainfall accumulation between the corresponding master and slave image acquisition dates. Two sudden drops in coherence are observed between master dates: 2015/08/15 and 2015/11/11. These are not associated with an increase in vegetation, temporal or perpendicular baselines but are related to rainfall accumulation.

However, as shown in Fig 3, rainfall accumulation between master and slave acquisitions was found to be associated with the sharp reduction in coherence. Rainfall leads to a disturbance and a dielectric change of the land surface which could have led to the coherence loss in this case.

SAR incidence angle and line of sight (LOS) is a final consideration influencing the DInSAR performance. A lower incidence angle leads to a higher spatial resolution, yet there is a real possibility of the subsidence signal being obscured by structures on the ground in the SAR's LOS [3]. Collecting data from descending and ascending satellite passes enables the observation of an area from the east and the west mitigating LOS challenges as well as providing the opportunity to collect three-dimensional deformation observations [4].

B. Geological Considerations

The final and more fundamental limitations are due to the nature of sinkhole precursors themselves. It is possible that no precursory deformation precedes a sinkhole development. The presence of chert bands in the study area, known for brittle failure with little warning [19], affects the potential for precursory deformation to be expressed. Furthermore, competent land cover types, like concrete, buildings or paved roads may be resistant to deformation and mask the expression of precursory deformation at the surface. Moreover, precursory deformation might only occur shortly before the sinkhole and deformation signatures are therefore masked by the sinkhole event depending on the temporal frequency of image acquisitions. Finally, the deformation magnitude may be too small to be detectable, especially in the presence of signal noise. In all these cases DInSAR would not be able to provide an early warning to sinkhole formation.

C. Concluding Remarks

The results of the investigation present evidence that precursory deformation prior to sinkhole development can be detected by conventional DInSAR techniques. It is expected that SAR and processing limitations can be overcome with advanced processing

techniques and appropriate SAR data selection. However, limitations related to the physical characteristics of sinkhole precursors remain a fundamental limitation to an early warning system based on ground deformation. Complementary ground-based methods are therefore expected to remain important for monitoring sinkhole prone land [9].

This investigation illustrates the opportunities and challenges to interferometric sinkholes precursor detection. There is a need for more evidence of DInSAR sinkhole precursors under different conditions. The resulting information will assist with the understanding of sinkhole dynamics as well as the operational limitations of DInSAR techniques in the context of a sinkhole early warning system.

Acknowledgment

The authors wish to thank the Council for Geoscience for providing the sinkhole inventory, the South African Weather Service for providing rainfall data and the Centre for Geographical Analysis at the Stellenbosch University for providing the SUDEM elevation model.

REFERENCES

[1] J. De Waele, F. Gutiérrez, M. Parise, and L. Plan, "Geomorphology and natural hazards in karst areas: A review," *Geomorphology*, vol. 134, no. 1–2, pp. 1–8, 2011.

[2] L. Chang and R. F. Hanssen, "Detection of cavity migration and sinkhole risk using radar interferometric time series," *Remote Sensing of Environment*, vol. 147, pp. 56–64, 2014.

[3] E. Intrieri, G. Gigli, M. Nocentini, L. Lombardi, F. Mugnai, F. Fidolini, and N. Casagli, "Sinkhole monitoring and early warning: An experimental and successful GB-InSAR application," *Geomorphology*, vol. 241, pp. 304–314, 2015.

[4] C. E. Jones and R. G. Blom, "Pre-event and post-formation ground movement associated with the Bayou Corne sinkhole," in *Proceedings of the Sinkhole Conference*, 2015, pp. 415–422.

[5] R. N. Nof, G. Baer, A. Ziv, E. Raz, S. Atzori, and S. Salvi, "Sinkhole precursors along the Dead Sea, Israel, revealed by SAR interferometry," *Geology*, vol. 4, no. 9, pp. 1019–1022, 2013.

[6] M. L. Rucker, B. B. Panda, R. A. Meyers, and J. C. Lommler, "Using InSAR to detect subsidence at brine wells, sinkhole sites, and mines," *Carbonates and Evaporites*, vol. 28, pp. 141–147, 2013.

[7] Z. Stevanovic, M. Parise, D. Closson, F. Gutiérrez, and Z. Stevanović, "Anticipating and managing engineering problems in the complex karst environment," *Environmental Earth Sciences*, vol. 74, pp. 7823–7835, 2015.

[8] J. P. Galve, C. Castanada, F. Gutirezz, and G. Herrera, "Assessing sinkhole activity in the Ebro Valley mantled evaporite karst using advanced DInSAR," *Geomorphology*, vol. 229, pp. 30–44, 2015.

[9] A. Ozden, A. Faghri, M. Li, and K. Tabrizi, "Evaluation of Synthetic Aperture Radar satellite remote sensing for pavement and infrastructure monitoring," *Procedia Engineering*, vol. 145, pp. 752–759, 2016.

[10] K. E. Joyce, S. Samsonov, S. R. Levick, J. Engelbrecht, and S. Belliss, "Mapping and monitoring geological hazards using optical, LiDAR, and synthetic aperture RADAR image data," *Natural Hazards*, vol. 73, no. 2, pp. 137–163, 2014.

[11] M. Parise, "A procedure for evaluating the susceptibility to natural and anthropogenic sinkholes," *Georisk: Assessment and Management of Risk for Engineered Systems and Geohazards*, vol. 9, no. 4, pp. 1–14, 2015.

[12] K. Terwel and R. F. Hanssen, "Predicting structural disasters with Radar interferometry," in *Proceedings of the International Association for Bridge and Structural Engineering Congress*, 2015, pp. 824–831.

[13] S. Richardson, "Sinkhole and subsidence record in the chuniespoort group dolomite , Gauteng , South Africa," Master's thesis. Pretoria: University of Pretoria, Department of Geology, 2013.

[14] A. Van Niekerk, "Stellenbosch University Digital Elevation Model (SUDEM)," in *Product description report (2013*

edition)., 2014, pp. 1–13.

[15] A. Theron, J. Engelbrecht, J. Kemp, W. Kleynhans, and T. Turnbull, "Detection of sinkhole precursors through SAR interferometry : first results from South Africa," in *Proceedings of the IEEE International Geoscience and Remote Sensing Symposium*, 2016.

[16] D. Massonnet and K. L. Feigl, "Radar interferometry and its application to changes in the Earth's surface," *Reviews of Geophysics*, vol. 36, no. 4, p. 441, 1998.

[17] A. Ferretti, A. Fumagalli, F. Novali, C. Prati, F. Rocca, and A. Rucci, "A new algorithm for processing interferometric data-stacks: SqueeSAR," *IEEE Transactions on Geoscience and Remote Sensing*, vol. 49, no. 9, pp. 3460–3470, 2011.

[18] J. Engelbrecht, C. Musekiwa, J. Kemp, and M. R. Inggs, "Parameters affecting interferometric coherence-the case of a dynamic agricultural region," *IEEE Transactions on Geoscience and Remote Sensing*, vol. 52, no. 3, pp. 1572–1582, 2014.

[19] D. J. Avutia, "Analytical and numerical study of dolomite sinkholes in Centurion, South Africa," Master's thesis. Cape Town: University of Cape Town, Department of Civil Engineering, 2014.

TABLE I
TERRASAR-X DATASET PROPERTIES

Acquisition date	Temporal baseline (days)[1]	Perpendicular baseline (metres)[1]
2015/01/29	11	217
2015/02/09	77	365
2015/04/27	11	341
2015/05/08	33	23
2015/06/10	11	41
2015/06/21	11	10
2015/07/02	11	69
2015/07/13	33	14
2015/08/15	22	3
2015/09/06	11	73
2015/09/17	11	4
2015/09/28	11	192
2015/10/09	11	12
2015/10/20	11	295
2015/10/31	11	271
2015/11/11	11	176
2015/11/22	11	184
2015/12/03	11	71
2015/12/14	22	57
2016/01/05	22	118
2016/01/27	N/A	N/A

[1]Relative to the following acquisition.

TABLE I
TERRASAR-X DATASET PROPERTIES
Table I
441x453mm (120 x 120 DPI)

TABLE II
DETAILS OF SINKHOLE INVENTORY EVENTS

Date	Type	Possible cause	D_x^* (m)	D_y^* (m)	D_z^* (m)
Mar 2015	Sinkhole	Leaking pipe	N/A	N/A	N/A
2015	Subsidence	Leaking pipe	16	4	0.2
2015	N/A	Leaking pipe	N/A	N/A	N/A
2015	Subsidence	Leaking pipe	N/A	N/A	N/A
3 Jan 2016	Sinkhole	Leaking pipe	20	13	9
Jan 2016	Sinkhole	Leaking pipe	6	3	2
29 Jan 2016	Sinkhole & Subsidence	Leaking sewer pipe	N/A	N/A	N/A

* D_x is the major axis diameter, D_y the minor axis diameter and D_z the depth.

TABLE II
DETAILS OF SINKHOLE INVENTORY EVENTS
Table II
465x308mm (120 x 120 DPI)

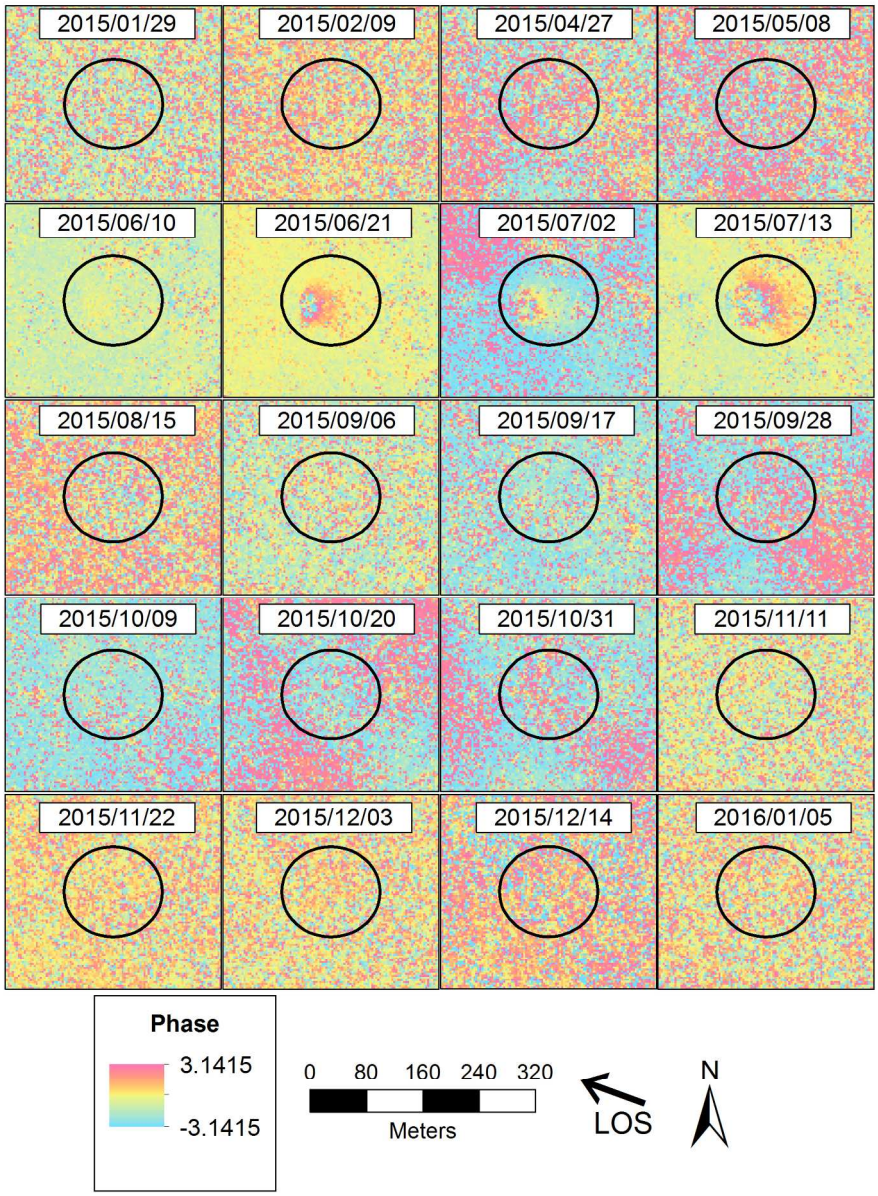

Fig. 1. Interferograms for the area surrounding the detected subsidence found within the black circle. Only the master date for each image pair is provided, the slave date of each image corresponds to the master date of the following image. The final slave date for the interferogram with the 2016/01/05 master is 2016/01/27. Deformation fringes are visible between 2015/06/21 and 2015/08/15.

Fig. 1
570x772mm (92 x 92 DPI)

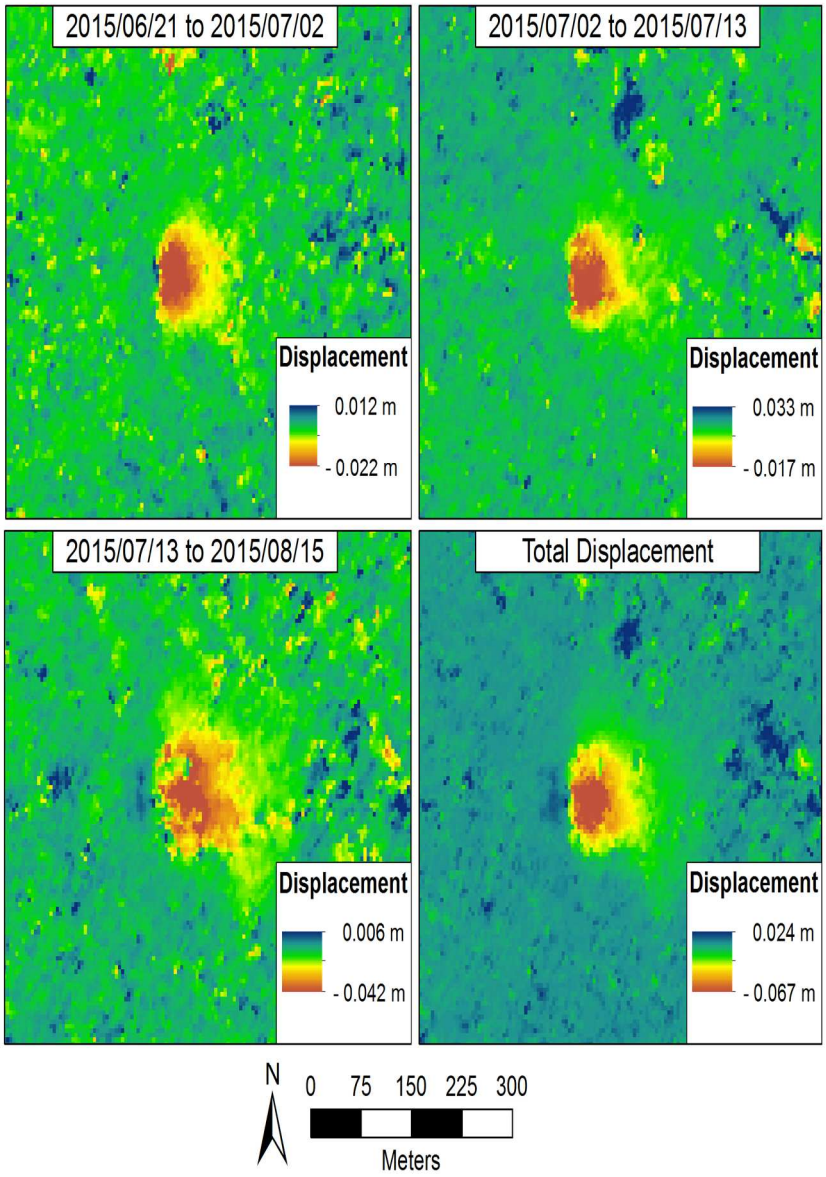

Fig. 2. Displacement maps of the deformation event derived from three interferograms as well as the sum of the three maps showing the total deformation detected over the period. The deformation gradient was steeper on the western periphery of the basin than on the east.
Fig. 2
820x793mm (64 x 94 DPI)

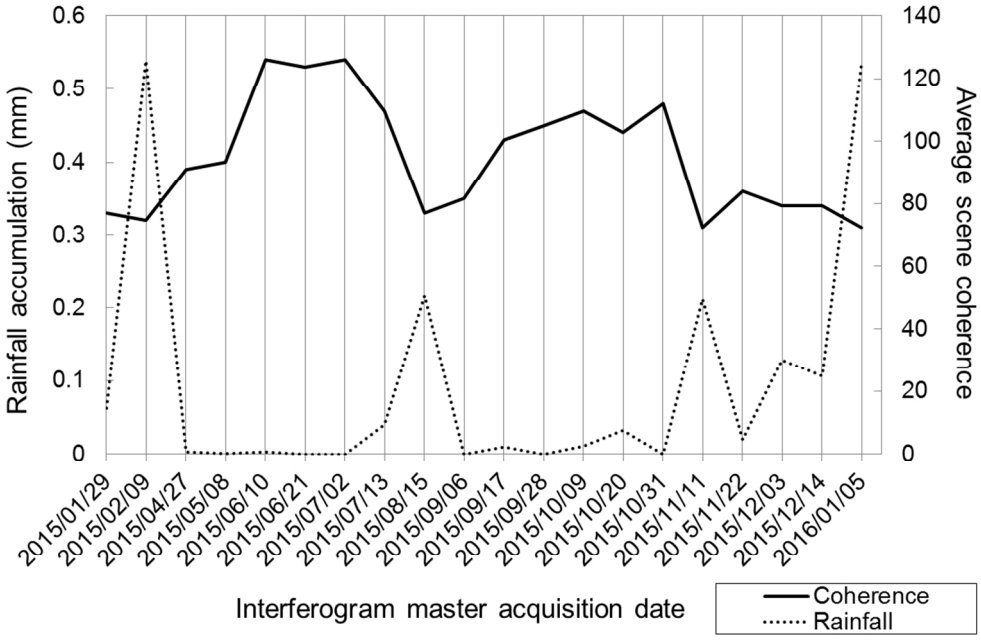

Fig. 3. Average global coherence and rainfall accumulation between the corresponding master and slave image acquisition dates. Two sudden drops in coherence are observed between master dates: 2015/08/15 and 2015/11/11. These are not associated with an increase in vegetation, temporal or perpendicular baselines but are related to rainfall accumulation.

Fig 3
206x135mm (150 x 150 DPI)